World Scientific Research Journal Volume 11 Issue 11, 2025
ISSN: 2472-3703 DOI: 10.6911/WSRJ.202511_11(11).0004

Effect of Transmission Shaft Offset on Conveyor Chain Vibration of Mesh Belt Dryer

Chi Zhang [1], Lin Dong [2,*], Yizhou Li [1]

[1] School of Mechanical Engineering, Xihua University, Chengdu 610039, China

[2] Institute of Modern Agricultural Equipment, Xihua University, Chengdu 610039, China

[*] Corresponding author: Lin Dong (Email: donglin11723@163.com)

Abstract

In order to investigate the influence of drive shaft offset on conveyor chain vibration in mesh belt dryer, the vibration of chain drive system is detected and analyzed by building a conveyor chain test platform, and at the same time, in order to better study the interaction between three factors, namely, rotational speed, center distance and offset, the response relationship of each factor on the transverse, longitudinal and lateral vibration displacements of the conveyor chain is analyzed by means of Box-Behnken test. It was found that when the test platform of conveyor chain was kept at the center distance of 660 mm, the level of triaxial vibration displacement increased with the increase of rotational speed; when the conveyor chain existed offset, the lateral vibration level of the test platform changed with the change of the tension level, i.e., the larger the average center distance of the two chains, the larger the amplitude of the lateral vibration displacement; when, in the rotational speed range from 27 rpm to 45 rpm, the rotational speed of 30 rpm When the rotational speed is 27 rpm to 45 rpm, the rotational speed is 30 rpm, the center distance is 659 mm, and the offset is 0 mm, the overall vibration amplitude of the conveyor chain test platform is the smallest, and the smoothness of the conveyor chain movement is the best. The study provides a reference for improving the smoothness of conveyor chain movement in mesh belt dryer.

Keywords

Conveyor Chain; Vibration; Mesh Belt Dryer; Test Platform.

1. INTRODUCTION

The mesh-belt dryer is a continuous food drying equipment for batch production. [1] By adding a mesh - belt conveyor chain inside the original box - type drying oven, continuous and uninterrupted drying can be achieved. [2] It is suitable for drying materials with high moisture content and good heat sensitivity, such as fruits, vegetables, etc. [3] However, during the manual adjustment and assembly of the conveyor chain, there is a situation where the left and right chains are unevenly tensioned, resulting in the inclination of the drive shaft and the non - coplanarity of the front and rear sprockets. [4] This causes abnormal vibration during the transmission of the conveyor chain, leading to an unsatisfactory drying effect of the products [5].

At present, some studies have been carried out. Mathematical models are established to simulate the lateral and longitudinal vibration behaviors of the chain span, as well as the torsional vibration characteristics of the sprockets. [6] A multi - body dynamics model of the balanced drive system of the driven sprocket is constructed to conduct torsional vibration analysis for optimizing parameter settings and reducing the vibration level in chain

ISSN: 2472-3703 DOI: 10.6911/WSRJ.202511_11(11).0004

transmission. A longitudinal dynamics model of chain transmission is built, and the finite element method is applied to analyze the longitudinal vibration modal frequencies of chain transmission. [7] However, the problem of the influence of the drive shaft offset on the stability of the conveyor chain system has received little attention [8].

In view of the above problems, this paper analyzes various factors affecting the running smoothness during the movement of the conveyor chain, explores the influence of rotational speed, center distance and offset on the vibration displacements of the conveyor chain in three axial directions, explores the range of three - axis vibration displacements during normal movement, provides a reasonable value range for various factors to maintain the smooth operation of the conveyor chain, prolongs the service life of the conveyor chain of the dryer, improves the transmission smoothness of the conveyor chain of the dryer, improves the product quality of the dryer, and enhances the market competitiveness of the enterprise's products.

2. THE STRUCTURE OF THE CONVEYOR CHAIN OF THE DRYER

The interior of the mesh - belt dryer consists of a cabinet, a fan, a heat pump, and a multi - layer mesh - belt conveying mechanism, as shown in Fig.1. [9] Each layer of the mesh - belt conveyor is composed of a mesh - belt, support pins, a motor, a reducer, a transmission shaft, bearings, sprockets, a roller conveyor chain, and a tensioning mechanism, as shown in Fig. 2. The mesh - belt is fixed between two chains by support pins to carry the materials. The motor is connected to the reducer, and the rotation is output through the transmission shaft. The sprockets are fixed at both ends of the transmission shaft, and the sprockets drive the chains to move the mesh - belt inside the cabinet.

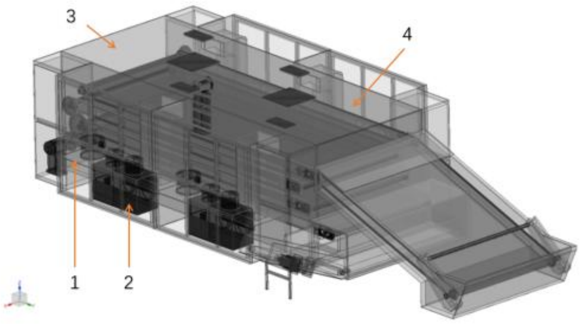

1-Fan; 2-Heat pump; 3-Cabinet; 4-Mesh - belt conveyor

Figure 1. Internal structure of mesh belt dryer

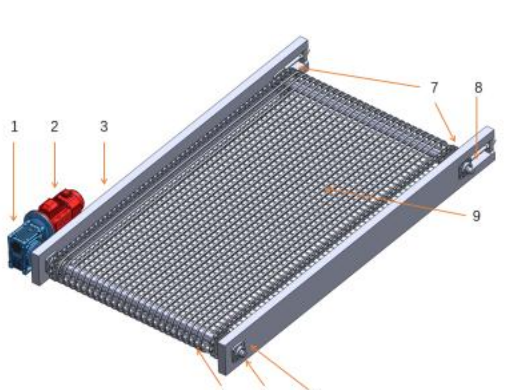

1-Reducer; 2-Electric motor; 3-Machine frame; 4-Support crossbar; 5-Drive shaft; 6-Bearing housing; 7-Double-pitch roller conveyor chain; 8-Tensioning mechanism; 9-Metal mesh belt

Figure 2. Basic structure of single-layer conveyor chain

ISSN: 2472-3703 DOI: 10.6911/WSRJ.202511_11(11).0004

3. CONSTRUCTION OF THE CONVEYOR CHAIN TEST PLATFORM

The main structure of the conveyor chain test platform consists of a frame, an electric motor, a reducer, sprockets, a frequency converter, chains, a drive shaft, bearings, and a tensioning mechanism, as shown in Fig. 3.

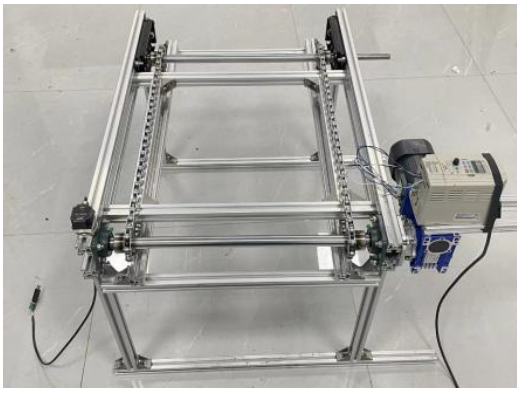

Figure 3. Conveyor chain test platform

3.1. Chain Selection for The Test Platform

The chain of the mesh-belt dryer selects the C208AL type double-pitch roller for transportation, and the chain material is 304 stainless steel. In order to restore the working condition of the conveyor chain of the mesh-belt dryer, the C2042HP type double-pitch hollow pin shaft chain with the same external geometric size is selected for the test platform. The pitch of both is 25.4mm, and the diameter of the roller is 15.88mm.

3.2. Sprocket Selection for The Test Platform

In order to match the chain model, the pitch of the C208AL type double-pitch roller chain for transportation is 25.4mm. For the test platform, the sprocket selected is a single-sided flanged sprocket with 8 teeth and of the 16A model, made of No. 45 steel, and the sprocket teeth are subjected to high-frequency quenching.

3.3. Motor And Reducer Selection

According to the characteristics of the drying materials, the variable-speed drying process, and the types of drying heat sources, the operating speeds of the conveyor chains on different layers of the multi-layer mesh-belt dryer are different and adjustable. Based on the operating speed range of 0.03 m/s to 0.15m/s of the conveyor chain of a certain type of mesh-belt dryer, the rotational speed range of the conveyor chain test platform can be obtained as 8.86 rpm to 44.29 rpm.

The formula for the tension when the conveyor chain meshes into the driving sprocket:

$$P = F_1 + F_2 \tag{1}$$

$$F_1 = 9.8(q_0 + q_1)\mu L_1 \tag{2}$$

$$F_2 = 9.8 q_0 \mu L_2 \tag{3}$$

In the equation: q_0 represents the weight per unit length of the mesh belt system; q_1 represents the weight of the material per unit length; μ represents the friction coefficient

ISSN: 2472-3703 DOI: 10.6911/WSRJ.202511_11(11).0004

between the mesh belt operating system and the guide rail; L_1, L_2 represent the lengths of the upper and lower guide rails.

The formula for the shaft power required to drive a single-layer conveyor chain system:

$$N_0 = \frac{P \times V}{102 \times 9.8} = \frac{(q_0 + q_1)wL_1 + q_0 wL_2}{102} \cdot V \tag{4}$$

Motor power formula:

$$N_c = K\frac{N_0}{\eta} = \left[\frac{(q_0 + q_1)wL_1 + q_0 wL_2}{102\eta}\right] \cdot V \tag{5}$$

In the equation, K is the motor starting coefficient; η is the mechanical transmission efficiency; V is the operating speed of the conveyor chain.

Substituting the data, we get N0 as 54W and NC as 108W.

Based on the above calculations, a 120W motor with a model of 5IK120A-YF can be selected, which has a rated speed of 1350 rpm. It is equipped with an RV040 worm gear reducer with a reduction ratio of 30. A VFD-M frequency converter is selected, and the input of the frequency converter is 0~50Hz, which can control the output shaft with an adjustable range of 0~45 rpm.

3.4. Selection Of Center Distance and Number of Chain Links for The Test Platform

The optimal center distance of chain drive is selected to be 30-50 times the pitch, and the maximum should not exceed 80 times the pitch. [10-13] A larger center distance will cause excessive sagging and suspension tension of the chain. For intermittent drives or drives with less than 17 teeth on the small sprocket, the center distance can be reduced to 20 times the chain pitch. [14] The test platform is a scaled model, with an estimated size of 750mm in length and 500mm in width. The center distance is designed to be selected within the range of 20 to 30 times the pitch. The number of teeth Z of the conveyor chain sprocket is 8, and the transmission ratio i = 1. If 26 times the pitch is initially selected, the initially selected center distance is 660mm.

The corresponding number of chain links X0 is:

$$X_0 = \frac{2a_0}{p} + Z \tag{6}$$

Substituting the data, we get: X0 is 59.968, then the number of chain links X is rounded up to 60.

3.5. Tensioning Mechanism Selection for The Test Platform

In order to facilitate the separate adjustment of the center distances of the two chains, the test platform uses a screw-type tensioning seat, as shown in Fig. 4. In the experiment, the tension degree of the chain is controlled by adjusting the center distance, and the adjustment range is 100mm. The UCF204 outer spherical square bearing with seat is selected for the bearing, and the shaft diameter is 20mm.

ISSN: 2472-3703 DOI: 10.6911/WSRJ.202511_11(11).0004

Figure 4. Screw-type tensioning seat

3.6. Three-axis Vibration Sensor

The three-axis vibration sensor of model WT-VB01-485 from Shenzhen Witmotion Technology Co., Ltd. is selected in the conveyor chain experimental platform. It is fixed on the profile bracket of the experimental platform through bolt connection, and the installation position is directly above the output shaft bearing. The sensor measurement is divided into X, Y, and Z three-axis directions. The X-axis direction is parallel to the output shaft direction, the Y-axis is parallel to the chain transmission plane, and the Z-axis is perpendicular to the conveyor plane. Its specific parameters are shown in Table 1.

Table 1. Basic Parameters Of WT-VB01-48 3-axis Vibration Transducer

Parameter Name	Value
Measurement Dimension	3-axis vibration displacement, 3-axis vibration velocity, 3-axis vibration frequency, 3-axis vibration angle
Measurement Range	Vibration displacement range 0 - 3000μm Vibration angle range 0 - 180° Vibration frequency range 1 - 100Hz Vibration velocity range 0 - 50mm/s
Output Frequency	100Hz (baud rate 230400) / 1Hz (baud rate 4800)
Measurement Accuracy	<F.S+5%
Working Voltage	5V-36V
Working Current	12mA

4. VIBRATION ANALYSIS OF THE CONVEYOR CHAIN TEST PLATFORM

4.1. Experimental Scheme Design

The experiment mainly explores the influence of three factors, namely rotational speed, center distance, and offset, on the vibration of the conveyor chain platform. The experimental scheme is mainly designed in the form of single-factor and multi-level, and mainly analyzes the lateral, longitudinal, and lateral vibration levels of the conveyor chain platform.
The experimental design scheme is as follows:

(1) To explore the influence of rotational speed on the vibration of the conveyor chain platform, in order to simulate the actual working conditions of the dryer conveyor chain, the rotational speed is set at five gradients by the control variable method, and the rotational speed of the driving wheel is set at 9rpm, 18rpm, 27rpm, 36rpm, and 45rpm.

(2) To explore the influence of the center distance on the vibration of the conveyor chain platform, the center distances are respectively set at 662mm, 660mm, and 658mm, and the center distances are measured by a laser rangefinder.

(3) To explore the influence of the offset on the vibration of the conveyor chain platform, the center distance ranges of the left and right chains are set at three tension levels of 658mm,

ISSN: 2472-3703 DOI: 10.6911/WSRJ.202511_11(11).0004

660mm, and 662mm, and their respective center distances are measured by a laser rangefinder to ensure accuracy, and the left and right offsets are respectively set at 2mm and 4mm.

4.2. The Influence of Rotational Speed on Conveyor Chain Vibration

Chain drive is a non-conjugate meshing drive with an intermediate flexible element. [15-18] To explore the influence of the rotational speed of the sprocket on the overall vibration level of the conveyor chain, this subsection of the experiment divides the rotational speed into 5 groups, and the experimental grouping is shown in Table 2. When the rotational speed of the driving wheel is at 9rpm, 18rpm, 27rpm, 36rpm, and 45rpm, the rotational speed of the mesh belt conveyor inside the dryer is simulated, where the center distance is 660mm, the center distances of the sprockets on both sides are the same, and the offset is 0. In the actual experiment, the smoothness of the conveyor chain platform transmission is examined through the average value of the three-axis vibration displacement exported by the three-axis vibration sensor, and the peak value of the three-axis vibration displacement is used to analyze whether there is abnormal meshing during the transmission process of the conveyor chain platform.

Table 2. Test grouping

Speed (rpm)	Center Distance (mm)	Offset (mm)
9	660	0
18	660	0
27	660	0
36	660	0
45	660	0

Under different rotational speeds, the changes in vibration displacement in the X, Y, and Z axis directions of the experimental platform are shown in Fig. 5. When the rotational speed remains stable, the vibration displacement situation begins to be recorded, and data is exported through the sensor, marking the peak and average values at different rotational speeds within 0s to 5s. It can be seen from the figure that in the interval from 0s to 5s, when the rotational speed increases from 9rpm to 45rpm, the peak and average values of the vibration amplitude of the X-axis generally increase with the increase of the rotational speed. The maximum vibration displacement peak value and the average value of the maximum vibration displacement both occur at a rotational speed of 45rpm, with the maximum vibration displacement being 47μm and the average vibration displacement being 12.918μm.

The peak and average values of the vibration amplitude of the Y-axis also generally increase with the increase of the rotational speed. The maximum vibration displacement peak value and the average value of the maximum vibration displacement both occur at a rotational speed of 45rpm, with the maximum vibration displacement being 42μm and the average vibration displacement being 14.878μm.

When the rotational speed increases from 9rpm to 45rpm, the peak and average values of the vibration amplitude of the Z-axis generally increase with the increase of the rotational speed. The maximum vibration displacement peak value and the average value of the maximum vibration displacement both occur at a rotational speed of 45rpm, with the maximum vibration displacement being 13μm and the average vibration displacement being 2.502μm.

Overall, under the condition of a theoretical center distance of 660mm, the vibration displacements of the three axes increase with the increase of speed, and the vibration displacements of the X-axis and Y-axis are basically at the same level, while the vibration displacement level of the Z-axis is relatively low.

ISSN: 2472-3703 DOI: 10.6911/WSRJ.202511_11(11).0004

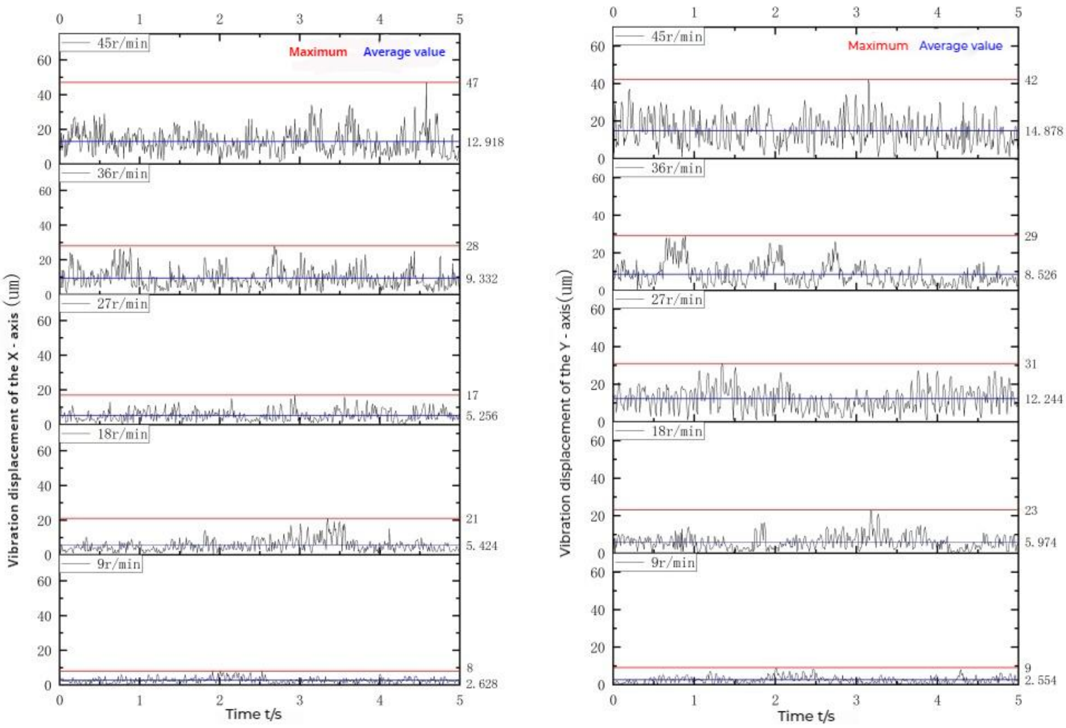

(a) Variation of X-axis vibration displacement (b) Variation of Y-axis vibration displacement

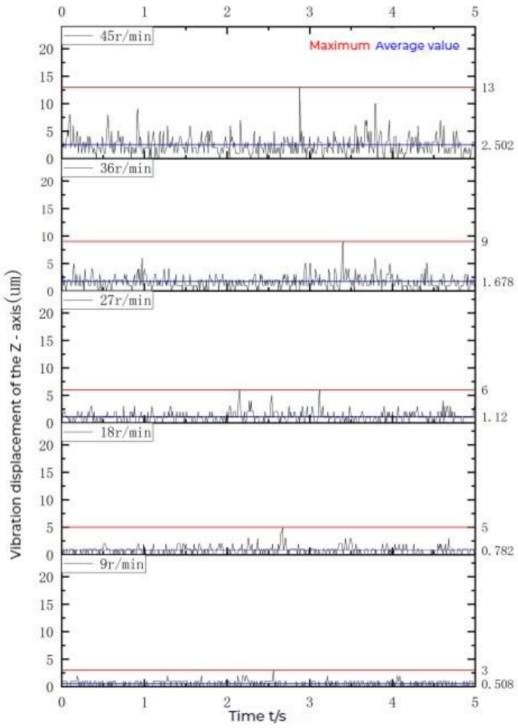

(c) Variation of Z-axis vibration displacement

Figure 5. Variation of X, Y and Z axis vibration displacements at different speeds for theoretical center distance

4.3. The Influence of Center Distance on Conveyor Chain Vibration

In order to explore the relationship between tension force and the overall vibration level of the conveyor chain, and to facilitate practical operation experiments, the tension level is characterized by controlling the center distance of the conveyor chain drive shaft. In this subsection, the three-axis vibration displacement at a center distance of 660mm will be compared. In the experiment, the screw tensioner will be adjusted from the original theoretical

ISSN: 2472-3703 DOI: 10.6911/WSRJ.202511_11(11).0004

center distance to 658mm to explore the influence of insufficient tension on the vibration of the conveyor chain platform; the screw tensioner will be adjusted to 662mm to explore the influence of excessive tension on the vibration of the conveyor chain platform. The rotational speed of the driving wheel is still set at five levels of 9rpm, 18rpm, 27rpm, 36rpm, and 45rpm, and the center distances of the sprockets on both sides are the same and the offset is 0.

The mean change in vibration displacement of the X, Y, and Z axes at five sets of rotational speeds for center distances of 658mm, 660mm, and 662mm is shown in Fig. 6. When the center distance is 662mm, both the mean and peak values of the lateral, transverse, and longitudinal vibration amplitudes are greater than those when the center distance is 660mm. This is because excessive tension increases the load on the tight side of the conveyor chain, which will cause the chain rollers on the tight side of the conveyor chain to lose contact with the supporting track, resulting in some rollers being suspended. Moreover, excessive tension will cause the chain to stretch and deform. Assuming that this stretching is evenly distributed on each link of the tight side, the actual pitch of each link will be greater than 25.4mm, resulting in greater impact when the driving and driven wheels mesh with the chain.

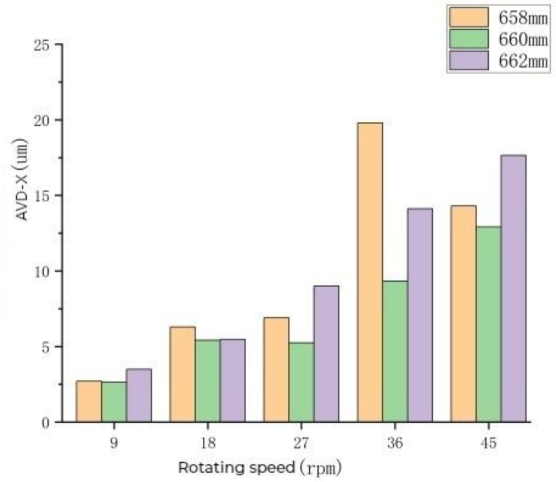

(a)Average vibration displacement of the X-axis

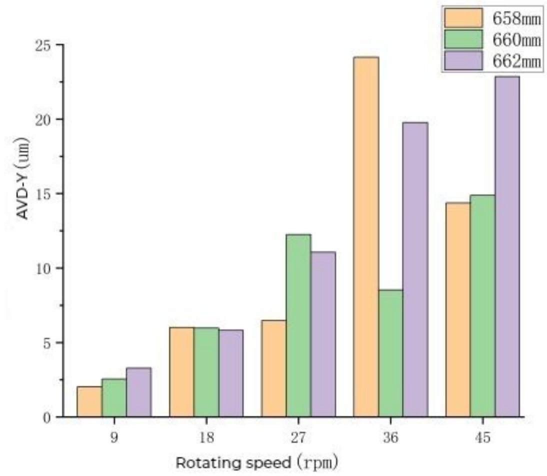

(b) Average vibration displacement of the Y-axis

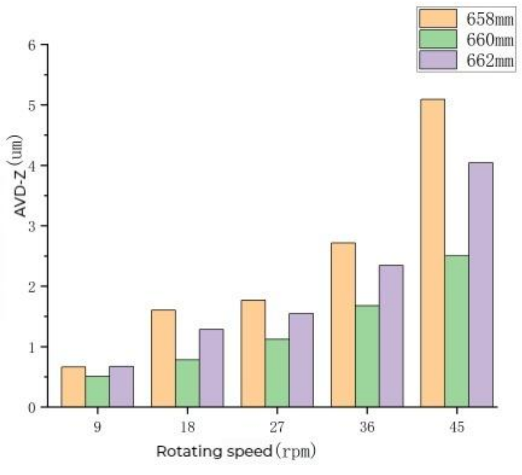

(c) Average vibration displacement of the Z-axis

Figure 6. Average vibration displacement of X, Y and Z axes with different center distance

4.4. The Influence of Drive Shaft Offset on The Lateral Vibration of The Conveyor Chain

First of all, in order to better distinguish the two chains, the conveyor chain near the motor and reducer in the experimental platform is called the left-end conveyor chain, and in contrast, the farther conveyor chain is called the right-end conveyor chain. The center distance ranges of

ISSN: 2472-3703 DOI: 10.6911/WSRJ.202511_11(11).0004

the left and right chains are set at three tension levels of 658mm, 660mm, and 662mm respectively, and the left and right offsets are 2mm and 4mm respectively. The distance between the left and right chains is 500mm. When the offset is 2mm, the offset angle of the driven wheel drive shaft is 6.981e-5 degrees. When the offset is 4mm, the offset angle of the driven wheel drive shaft is 1.396e-4 degrees. A total of 6 groups of experiments are designed, and the experimental grouping is shown in Table 3.

Table 3. Test grouping

Test Number	Left Center Distance (mm)	Right Center Distance (mm)	Offset (mm)
1	658	660	2
2	660	658	2
3	662	660	2
4	660	662	2
5	658	662	4
6	662	658	4

In Fig. 7, for Test Group 1, when the rotational speed ranges from 9rpm to 45rpm, the peak and average values of the vibration amplitude of the X-axis generally increase with the increase of the rotational speed. The maximum vibration displacement peak value and the average value of the maximum vibration displacement both occur at a rotational speed of 45rpm, with the maximum vibration displacement being 52μm and the average vibration displacement being 16.024μm. For Test Group 2, the maximum vibration displacement peak value and the average value of the maximum vibration displacement both occur at a rotational speed of 36rpm, with the maximum vibration displacement being 40μm and the average vibration displacement being 13.856μm. For Test Group 3, the maximum vibration displacement peak value and the average value of the maximum vibration displacement both occur at a rotational speed of 45rpm, with the maximum vibration displacement being 63μm and the average vibration displacement being 21.4μm. For Test Group 4, the maximum vibration displacement peak value and the average value of the maximum vibration displacement both occur at a rotational speed of 45rpm, with the maximum vibration displacement being 44μm and the average vibration displacement being 16.724μm. Through a systematic comparison of the lateral vibration displacement amplitudes of the experimental platform, this study delves into the impact of varying center distances on the vibration level of a belt drive system under a specific axial offset condition. The experimental data clearly reveal a regular pattern: under the operating condition where the driven wheel has a 2mm axial offset, the lateral vibration level of the experimental platform shows a significant positive correlation with the center distance. Specifically, the vibration displacement amplitudes of Test Groups 3 and 4 are markedly higher than those of Test Groups 1 and 2, which in turn are higher than the baseline case with a 660mm center distance and no offset. Based on this, the paper concludes that when the axial offset is 2mm, an increase in the center distance leads to the intensification of the system's lateral vibration. This finding holds significant guiding implications for the optimal design and fault diagnosis of belt drive systems. the axial offset acts as the "excitation source" for the vibration. When a 2mm axial offset exists in the driven wheel, the motion plane of the transmission belt is forced to twist and deflect as it wraps onto and off the wheel. This periodic geometric interference is equivalent to applying a continuous lateral excitation force to the belt system, thereby exciting the belt's own lateral vibration and the coupled vibration of the entire experimental platform. Therefore, the entire process can be understood as follows: the axial offset sets the "tone" of the vibration, while the center distance plays the role of an "amplifier." With the excitation source held constant, the increase in system stiffness paradoxically leads to a more intense vibration output, due to the simultaneous increase in the amplitude of the excitation force.

ISSN: 2472-3703 DOI: 10.6911/WSRJ.202511_11(11).0004

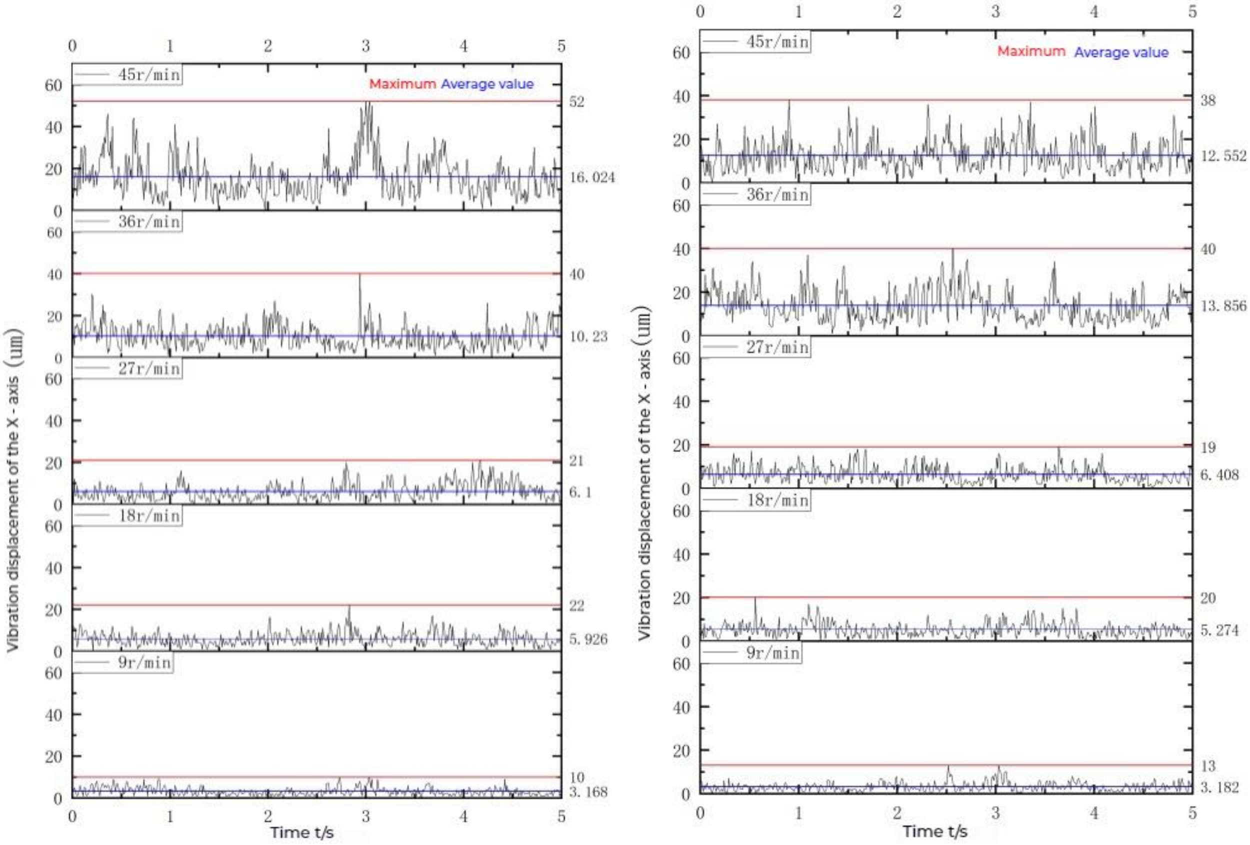

(a) Variation of vibration displacement of the X-axis in Group 1 (b) Variation of vibration displacement of the X-axis in Group 2

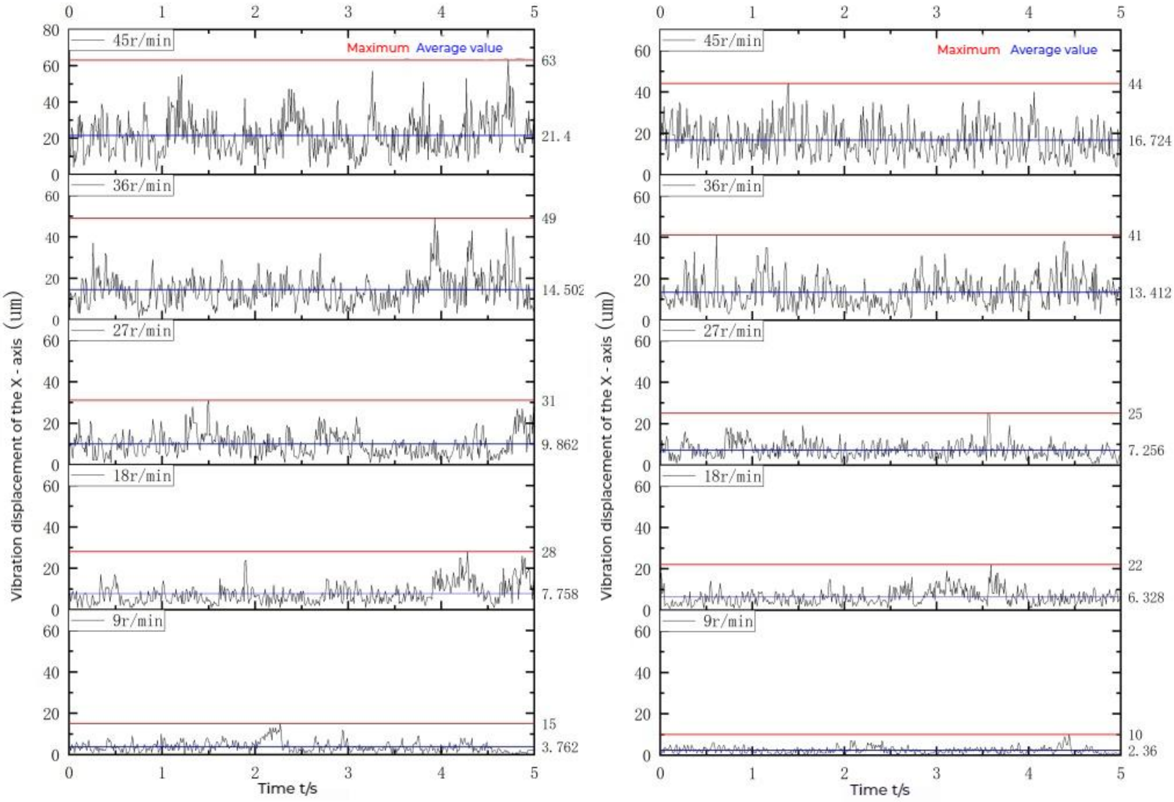

(c) Variation of vibration displacement of the X-axis in Group 3 (d) Variation of vibration displacement of the Group 4's X-axis

Figure 7. Amplitude of lateral vibration of conveyor chain at 2mm center distance offset

ISSN: 2472-3703 DOI: 10.6911/WSRJ.202511_11(11).0004

In Fig. 8, for Test Group 5, the maximum vibration displacement peak value and the average value of the maximum vibration displacement both occur at a rotational speed of 36rpm, with the maximum vibration displacement being 34μm and the average vibration displacement being 13.544μm. For Test Group 6, the maximum vibration displacement peak value and the average value of the maximum vibration displacement both occur at a rotational speed of 45rpm, with the maximum vibration displacement being 36μm and the average vibration displacement being 13.036μm. In the case of an axial offset of 4mm of the sprocket, the two center distances of the two groups of tests on the left and right are symmetrically arranged. By comparing the vibration displacements of Test Groups 5 and 6 with those at a center distance of 660mm without offset, it can be inferred that the lateral vibration level of the test platform does not significantly increase. This is determined by the average tension level of the left and right chains of the test platform, that is, the average center distance of the two chains is 660mm, and the closer the average center distance is to the theoretical center distance, the smaller the vibration amplitude.

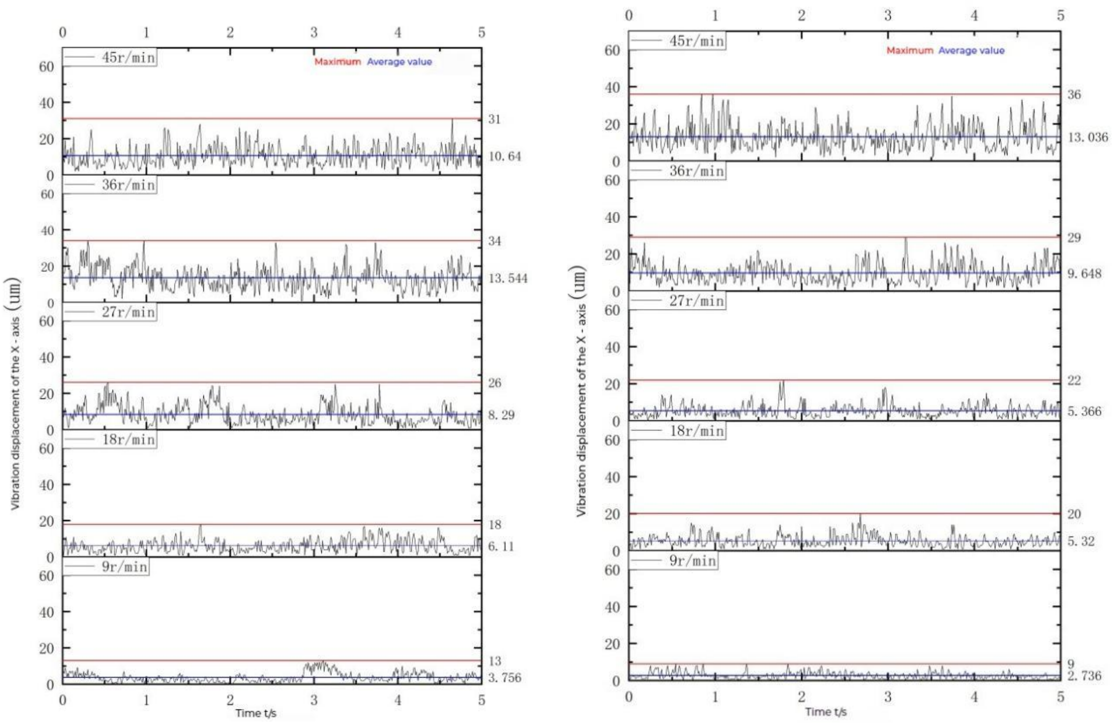

(a) Variation of vibration displacement of the X-axis in Group 5 (b) Variation of vibration displacement of the X-axis in Group

Figure 8. Amplitude of lateral vibration of conveyor chain at 4mm center distance offset

5. THE INFLUENCE OF THE INTERACTION OF THREE FACTORS ON CONVEYOR CHAIN VIBRATION

5.1. Response Surface Design and Experimental Results

In order to analyze the influence degree of various factors more scientifically and intuitively, the Design-Expert 11 software is used to design a response surface experiment, that is, the Box-Behnken experiment. In order to better study the interaction influence among the three factors of rotational speed, center distance, and offset, the response relationship of each factor to the lateral, longitudinal, and lateral vibration displacements of the conveyor chain is analyzed by the response surface method. A three-factor and three-level experimental scheme will be designed, taking the average vibration displacements in the lateral, longitudinal, and transverse directions as response values.

ISSN: 2472-3703 DOI: 10.6911/WSRJ.202511_11(11).0004

5.1.1. Response surface analysis of lateral vibration displacement

When studying the influence of the interaction of two factors on the index, the intermediate level is selected for the additional factor. The response surface and contour plots of the influence of the interaction of the driving wheel speed (A), center distance (B), and offset (C) on the lateral average vibration displacement (X) are shown in Fig. 9.

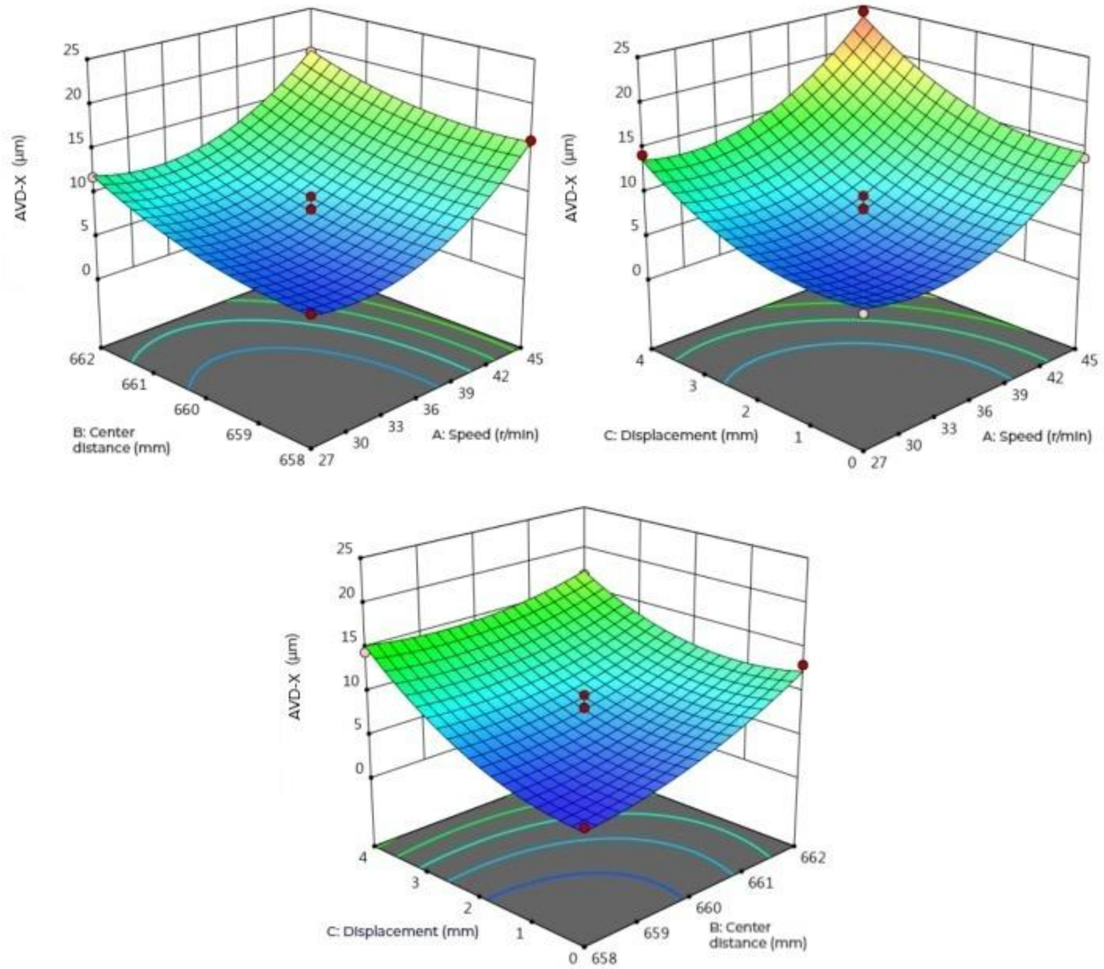

(a) Response surface plot of the influence of the interaction between A and B on X (b) Response surface plot of the influence of the interaction between A and C on X (c) Response surface plot of the influence of the interaction between B and C on X

Figure 9. Response surface curve graph of lateral average vibration displacements

It can be seen from the steepness of the response surface in Fig. 9 that the magnitude of the influence of the interaction between two factors (AB, AC, BC) on the lateral average vibration displacement is in the following order: BC > AC > AB. Among them, the interaction between the center distance and the offset has a significant influence on the lateral average vibration displacement ($P < 0.05$), while the interaction between the driving wheel speed and the offset is not significant, and neither is the interaction between the driving wheel speed and the center distance.

5.1.2. Response Surface Analysis of Longitudinal Vibration Displacement

The response surface and contour plots of the influence of the interaction of the driving wheel speed (A), center distance (B), and offset (C) on the longitudinal average vibration displacement (Y) are shown in Fig. 10.

ISSN: 2472-3703 DOI: 10.6911/WSRJ.202511_11(11).0004

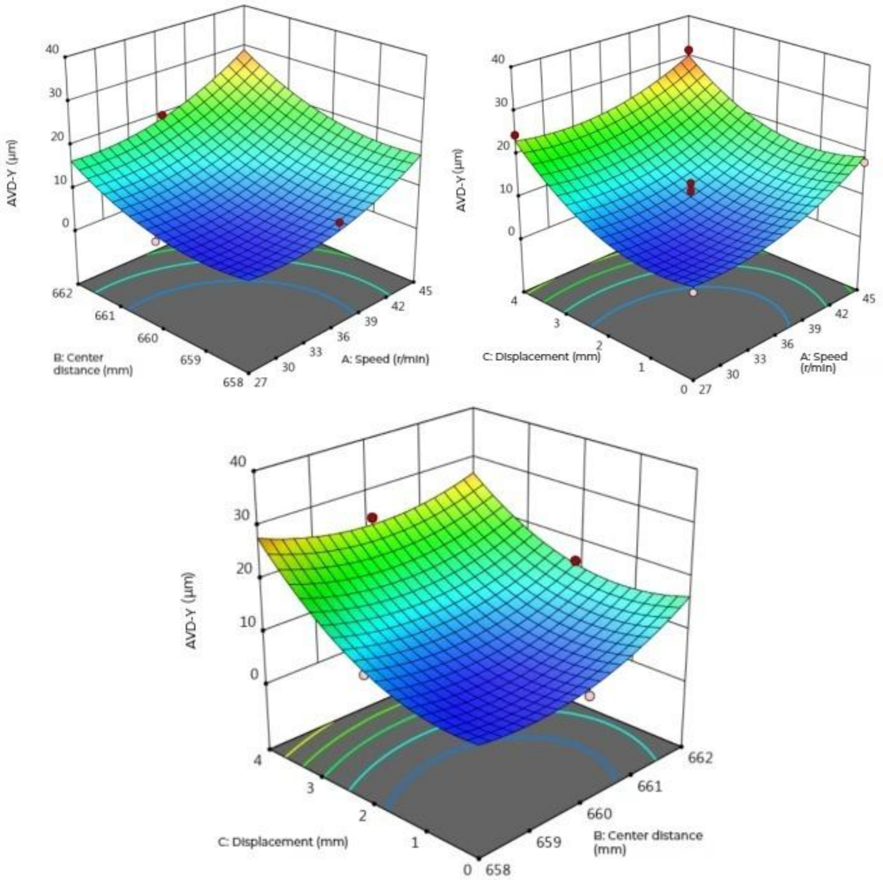

(a) Response surface plot of the influence of the interaction between A and B on Y (b) Response surface plot of the influence of the interaction between A and C on Y (c) Response surface plot of the influence of the interaction between B and C on Y

Figure 10. Response surface curve graph of longitudinal average vibration displacements

It can be seen from the steepness of the response surface that the magnitude of the influence of the interaction between two factors (AB, AC, BC) on the longitudinal average vibration displacement is in the order of BC > AC > AB, but the interaction of all three factors is not significant.

5.1.3. Response Surface Analysis of Transverse Vibration Displacement

The response surface and contour plots of the influence of the interaction of the driving wheel speed (A), center distance (B), and offset (C) on the transverse average vibration displacement (Z) are shown in Fig. 11.

ISSN: 2472-3703 DOI: 10.6911/WSRJ.202511_11(11).0004

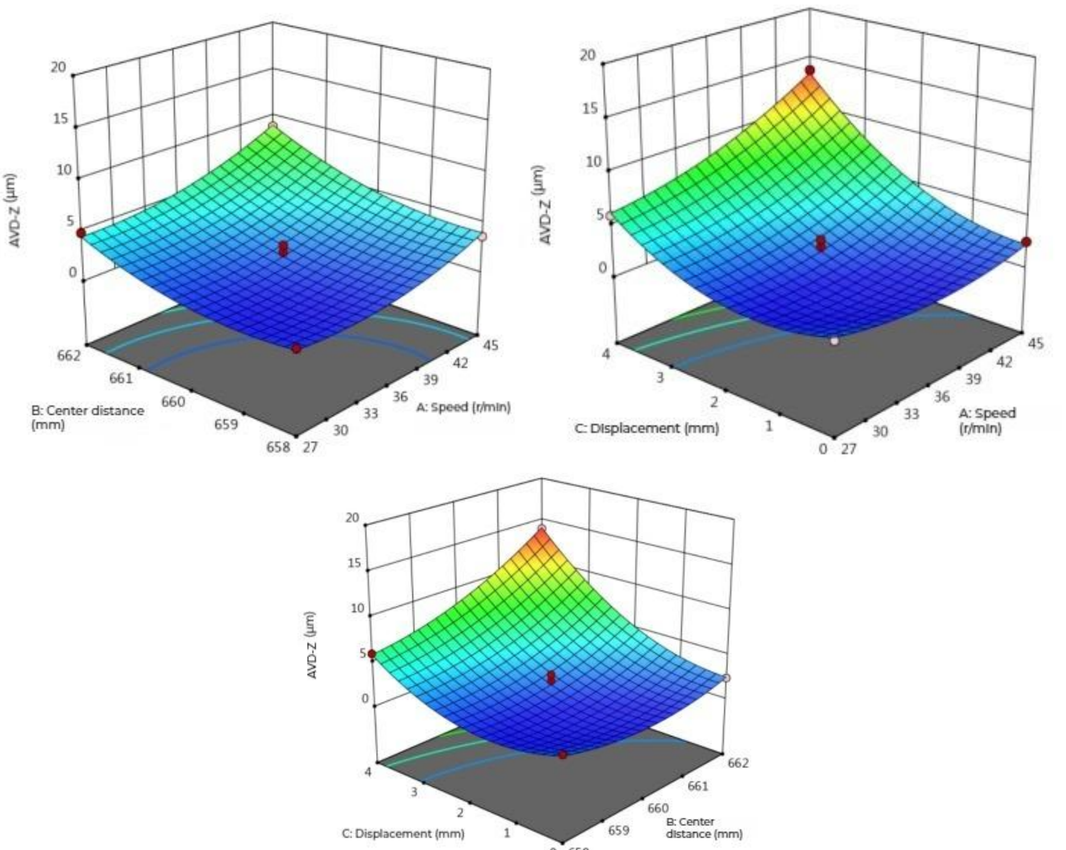

(a) Response surface plot of the influence of the interaction between A and B on Z (b) Response surface plot of the influence of the interaction between A and C on Z (c) Response surface plot of the influence of the interaction between B and C on Z

Figure 11. Response surface curve graph of transverse average vibration displacements

It can be seen from the steepness of the response surface that the magnitude of the influence of the interaction between two factors (AB, AC, BC) on the transverse average vibration displacement is in the order of BC > AC > AB. Among them, the interaction between the center distance and the offset and the interaction between the driving wheel speed and the offset have a significant influence on the lateral average vibration displacement ($P < 0.05$), while the interaction between the driving wheel speed and the center distance is not significant.

5.2. Optimization Results and Verification

The ideal value of the response index required by the test is that the lateral, longitudinal, and transverse vibration displacements of the conveyor chain are simultaneously minimized. The constraint conditions setting and optimization results are shown in Table 3. The optimal level combination optimization results show that when the rotational speed is 30.717 r/min, the center distance is 659.172 mm, and the drive shaft offset is 0.14834 mm, the results of each test index are the best, namely: lateral average vibration displacement: 4.699 μm, longitudinal average vibration displacement: 6.608 μm, and transverse average vibration displacement: 1.016 μm.

The final optimization results are verified. A verification test is carried out when the rotational speed is 30 r/min, the center distance is 659 mm, and the drive shaft offset is 0 mm. The verified mean value of the lateral vibration displacement is 4.821 μm, with a relative error of 2.5%; the mean value of the longitudinal vibration displacement is 6.724 μm, with a relative error of 1.8%; and the mean value of the transverse vibration displacement is 1.124 μm, with a relative error of 10.5%. This indicates that the equation has a good degree of fitting.

ISSN: 2472-3703 DOI: 10.6911/WSRJ.202511_11(11).0004

Table 4. Optimize the constraints and goal Settings

Name	Goal	Lower Limit	Upper Limit	Lower Weight	Importance
A	Is in range	27	45	1	3
B	is in range	658	662	1	3
C	is in range	0	4	1	3
X	minimize	4.53	24.32	1	3
Y	minimize	6.48	31.56	1	3
Z	minimize	0.98	13.98	1	3

6. CONCLUSION

In response to the instability phenomenon of the conveyor chain of the mesh belt dryer in actual operation, this paper takes the single-layer conveyor chain transmission system in the mesh belt dryer as the research object. First, the structure of the single-layer conveyor chain transmission is analyzed in detail, and then a small conveyor chain test platform is designed and built to study the changes in the lateral, longitudinal, and lateral vibration displacements of the conveyor chain platform caused by the rotational speed, center distance, and offset. Finally, through the Box-Behnken test, with the average vibration displacement as the response value, the interaction effects of the chain rotational speed, center distance, and offset on the lateral, longitudinal, and lateral vibrations of the test platform and their quadratic regression models are analyzed. The research in this paper has certain guiding significance for improving the smoothness of the conveyor chain motion.

This paper has built a small test prototype for the roller conveyor chain transmission system and focused on the study of the influence of the drive shaft offset on the vibration amplitude of the conveyor chain system. However, in actual working conditions, the temperature rise in the dryer will cause the chain to elongate, and the influence of temperature on the conveyor chain transmission can be further analyzed in future research.

ACKNOWLEDGMENT

The authors declare that there is no conflict of interest in preparing this paper.

This research was funded by the Key R & D Projects of the Sichuan Provincial Department of Science and Technology of China (Grant No.: 2023YFG0049, 2022YFG0065) and the Project of the Sichuan Modern Agricultural Equipment Engineering Technology Research Center of China (Grant No.: XDNY2021-003).

REFERENCES

[1] Chenyang, Z. and Yanxia, S.A 2-DOF-IMC method for suppressing transmission chain vibration of wind power generation system with a clearance, Advances in Mechanical Engineering., 14, 2022.

[2] Huan, Z. and Lin, D., et al. Design of Intelligent Control System for Multi-material and Widely Compatible Mesh Belt Dryer, Sichuan Agriculture and Agricultural Machinery., 5,22-25, 2023.

[3] Gongzhong, L. and Pengkai, W., et al. Analysis of heat flow field and structure optimization of multi-temperature zone mesh belt dryer, Journal of Agricultural Engineering., 37(18), 40-47, 2021.

[4] Kai, W. and Yong, L., et al. Dynamic characterization of roller chains under high-speed continuous strong impact, Vibration and Shock., 41(15), 280-286, 2022.

[5] Jiang, S. B. and Huang, S., et al. Dynamic properties of chain drive system considering multiple impact factors, International Journal of Simulation Modelling., 21,2 84-295, 2022.

ISSN: 2472-3703 DOI: 10.6911/WSRJ.202511_11(11).0004

[6] Ren, W. J. and Wang, L., et al. Coupling properties of chain drive system under various and eccentric loads, International Journal of Simulation Modelling.,19,643-654, 2020.

[7] Yu, W. G. Research on longitudinal dynamics of chain drive, Machinery Manufacturing., 58(06), 37-40, 2020.

[8] Chen, C. H.Research on numerical simulation of temperature field and structural optimization of mesh belt dryer for oil tea seeds, Central South Forestry University of Science and Technology. 2020.

[9] Yan, J. F.Research and application of mesh belt dryer, Agricultural Machinery Use and Maintenance., 2, 65-67, 2023.

[10] Lu, L. and Lu, J. P. Research on flattening technology and device design of monkey kui tea, Packaging and Food Machinery., 39(05), 62-67, 2021.

[11] Shi, Q. and Zhou, Y. B., et al. Design of synchronization monitoring system for double chain drive of chain harrow pickup mechanism, Chinese Journal of Agricultural Mechanical Chemistry., 42(11), 7-11, 2021.

[12] Jiang, J. P. and Dong, H. Y., etal. Design and test of 9QQ1600-5 silage reclaimer, Agricultural Mechanization Research., 44(09), 55-62, 2022.

[13] Zhou, Y. B. and Zhou, H. P., etal.Design of chain harrow residual film recycling machine chain drive fault monitoring system, Agricultural Mechanization Research., 44(10), 82-87, 2022.

[14] Shen, S. L. and Wang, D. W., et al. Design and experimental study of a side spread harvester for Salvia divinorum, Agricultural Mechanization Research., 43(05), 135-139, 2021.

[15] Zhang, S. P. and Tak, T. O. Efficiency estimation of roller chain power transmission system, Applied Sciences., 10(21), 2020.

[16] Fuglede, N. and Thomsen, J. J. Kinematic and dynamic modeling and approximate analysis of a roller chain drive, Journal of Sound and Vibration., 366, 447-470, 2016.

[17] Kou, B. and Liu, Q. Research on transverse vibration characteristics of rope change device with clamping chain transmission in lifting system, Journal of Vibroengineering., 19(2), 894-907,2017.

[18] Ambrosio, J. and Malça, C. Planar roller chain drive dynamics using a cylindrical contact force model, Mechanics Based Design of Structures and Machines., 44(1-2), 109-122, 2016.